Lab on a Chip

Accepted Manuscript

ROYAL SOCIETY OF CHEMISTRY

www.rsc.org/loc

Title: Paired single cell co-culture microenvironment isolated by two-phase flow with continuous nutrient renewal

Author affiliation:

Yu-Chih Chen[1], Yu-Heng Cheng[1], Hong Sun Kim[2], Patrick N Ingram[3], Jacques E. Nor[2,3] and Euisik Yoon[1,3]

[1]Department of Electrical Engineering and Computer Engineering, University of Michigan, 1301 Beal Avenue, Ann Arbor, MI 48109-2122;

[2]Department of Cariology, Restorative Sciences, Endodontics, School of Dentistry, University of Michigan;

[3]Dept. of Biomedical Engineering, University of Michigan, Ann Arbor, MI, USA, 2200 Bonisteel, Blvd. Ann Arbor, MI 48109-2099.

Corresponding author:

Euisik Yoon, 1301 Beal Avenue, Ann Arbor, MI 48109-2122, 734-615-4469, esyoon@umich.edu.

Abstract:

Cancer-stromal cell interaction is a critical process in tumorigenesis. Conventional dish-based assays, which simply mix two cell types, are limited in three aspects: 1) Limited control of cell microenvironment; 2) Inability of studying cell behavior in a single-cell manner, and; 3) Difficulties in characterizing single cell behavior within a highly heterogeneous cell population (e.g. tumor). An innovative use of microfluidic technology is centered on improving the spatial resolution for single cell assays. However, it is challenging to isolate the paired interacting cells, while maintaining nutrient renewal. In this work, two-phase flow was used as the simple isolation method, separating the microenvironments of each individual chamber. As nutrients in an isolated chamber are consumed by cells, media exchange is required. To connect cell culture chamber to the media exchange layer, we demonstrated a 3D microsystem integration technique using vertical connections fabricated by deep reactive-ion etching (DRIE). Compared to previous approaches, the presented process allows the area reduction in vertical connections by an order of magnitude, enabling compact 3D integration. A semi-permeable membrane was sandwiched between cell culture layer and media exchange layer. The selectivity of the semi-permeable membrane can retain the signaling proteins within the chamber, while allowing free diffusion of nutrients (e.g., glucose and amino acids). Thus, paracrine signals are accumulated inside the chamber without cross-talk with cells in other chambers. Utilizing these innovations, we demonstrated co-culture of UM-SCC-1 (head and neck squamous cell carcinoma) cells and endothelial cells to recapitulate tumor proliferation enhancement in the vascular endothelial niche.

Keywords:

Cell-cell Interaction, pairing single cells, Co-culture, two-phase isolation, semi-permeable membrane, 3D integration, DRIE.

Introduction:

The cancer cell niche is a complex microenvironment where cancer cells, endothelial cells (EC), macrophages, and mesenchymal stem cells (MSC) coexist,[1] and tumor-stromal cell interactions can determine the development of the tumor.[2] It is believed that tumor cells exploit nearby normal cells to

enhance growth, metastasis, and drug resistance. Conventionally, cell interactions can be studied by co-culturing two different cell types in the same petri dish. However, this dish based co-culture model lacks several key aspects to comprehensively understand cancer development. First, metastatic cancer cells typically metastasize as single circulating tumor cells (CTC); therefore, single-cell-derived tumorigenesis may be different from what is observed when co-culturing many cells.[3,4] Second, conventional dish culture cannot provide an accurate model of tumorigenesis processes, as cell behavior will be affected by uncontrolled interaction with multiple neighboring cells.[5] In conventional interaction assays, two cell populations are simply mixed in a dish, so the spatial distribution of two cell types is not uniform, resulting in significant variation between locations. Some cells may be surrounded by many of the other type of cells in one region, while others may aggregate with the same type of cells in another region. As such, it is difficult to achieve precise ratio controlled co-culture in the conventional culture platforms. Third, dish-based culture lacks the ability to use small samples (<1,000 cells). This is important because it is difficult to acquire large samples of CTCs or primary samples. Finally, for highly heterogeneous populations such as cancer, dish-based co-culture can only monitor the average behavior, rather than tracking individual cell behavior. This can be an issue because some sub-populations in tumors have different metastasis potential. Although microfluidic technology provides better control over co-culture microenvironment, many platforms still load hundreds or thousands of cells in the device, so they lack single cell resolution as conventional co-culture in petri dishes.[6-14]

Although the single cell co-culture on-chip allows for isolating single cells in the chamber, there are still two critical issues to be resolved: 1) Due to the small amount of secreted proteins from single cell, continuous perfusion can easily wash away the secretion and thus impair cell-cell interaction; and 2) As the platform aims to study the heterogeneity of single cells, the chamber-chamber cross-talk, which can cause undesired interaction, should be eliminated. In the previous works reported on the single cell-cell interaction[15,16], the co-culture microenvironment of each cell group was not completely isolated. Thus, the cross-talk among different co-culture environments can inevitably distort the cell behaviors. Droplet based technology can naturally provide isolated co-culture microenvironment at single cell level;[17-19] however, droplet based cell culture is limited in the study of mammalian cells. First, most mammalian cells are adherent cells; therefore, suspension in a droplet can lead to anoikis, resulting in cell apoptosis.[20] Second, it is difficult to continuously provide fresh media to each droplet, so the nutrition in the isolated droplet depletes over time. Previously, our group reported two different platforms, which are capable of controlling the isolation time of paired cells by pneumatic valve or electrolytic bubble generation and removal.[21,22] In these platforms, the isolation time was optimized based on the accumulation of signaling proteins and nutrition depletion.

Nevertheless, it is difficult to determine the optimal cell interaction time, especially for cancer cells, a highly heterogeneous population. Cells with low metabolism rates, which are likely to be quiescent and drug resistant, may need longer interaction times, while high metabolism rate cells, which contribute to rapid growth, may need a short interaction time. In order to fully characterize the sub-populations in the tumor, we should not miss any sub-population behaviors. In addition, the difference in proliferation rates after culturing several days (some chambers with more cells and others with less cells) will make the situation even more complicated.

In this work, we used a semi-permeable membrane for cell-cell interaction studies. The semi-permeable membrane under each micro-chamber can provide stable nutrient supply for cells, while retaining the secreted signaling proteins for interaction, without using any external control mechanisms

for micro-chamber isolation. We incorporate immiscible oil isolation to achieve stable channel isolation in a simple and robust way. As a result, the device can operate without any external components such as micropumps or electrical control signals. For proof of feasibility, we demonstrated the interaction between UM-SCC-1 (head and neck squamous cell carcinoma) cells and endothelial cells (EC). Secreted cytokines from ECs can boost the growth of UM-SCC-1 cells as compared to control experiments where UM-SCC-1 cells were cultured alone.

Materials and Methods

Microfluidic Device Operation

The presented platform provides three functions: pairing of single cells for co-culture, oil isolation to avoid the cross-talk between chambers, and nutrient renewal through the semi-permeable membrane. To pair single cells, the hydrodynamic cell capture scheme is implemented. Using two capture sites per chamber, two cells can be captured in the same chamber as shown in Fig. 1 (A). After cell capture, the chambers are isolated by an immiscible oil phase. The oil flows left to right, so the cell chambers sandwiched by two parallel oil channels are isolated (Fig. 1 (B)). The nutrition can be supplied to the cells in the isolated chamber through the semi-permeable membrane (2k Daltons Cut-off molecular weight), while the secreted cytokines are accumulated inside the chamber because their molecule sizes (typically tens of kDa) are too large to escape (Fig. 1 (C)). In this manner, secreted cytokines are retained inside the chamber for cell-cell interaction, while the nutrition can be steadily supplied through a semi-permeable membrane.

Device Fabrication

Three layers (cell culture layer, substrate with vertical connections, and the media exchange layer) were fabricated separately, and then all three layers were aligned and bonded (Fig. S1). For the cell culture layer, three masks were used to fabricate a SU8 (Microchem) master mold: the first mask for a shallow (10 μm) interaction bridge, the second mask for microfluidic channels and cell culture chambers (40 μm), and the third mask for oil isolation channels (100 μm). The PDMS (PDMS, Sylgard 184, Dow Corning) layer was fabricated using the standard soft lithography processes. We used a 100 μm-thick fused silica wafer (Fused silica wafer, University wafer, MA) for substrate. In order to form vertical connections, a 50μm SU-8 layer was spin-coated and patterned and used as the mask for DRIE. The fused silica was etched through by DRIE (Pegasus glass etcher), and the residual SU-8 was removed by PG Remover (Microchem). The media exchange channel was formed by HF etching of a glass substrate. The media exchange layer has many pillars (100 μm by 100 μm) to support the semi-permeable membrane (Dialysis Membrane 2K MWCO, Fisher Scientific) on top, and the images of semi-permeable membranes are shown in Fig. S2. The PDMS channel layer and the vertical connection layer were treated with oxygen plasma and then aligned and bonded together. Finally, the bonded PDMS-fused silica, semi-permeable membrane, and media exchange layer were all assembled and sealed utilizing UV cured Epoxy (OG147, Epoxy technology).

Cell Culture Experiment

UM-SCC-1 cells were cultured with DMEM (Gibco 11965), 10% FBS (Gibco 10082), and 1% Pen/Strep (Gibco 15140), and human dermal microvascular endothelial cells were cultured with EGM-2 (Lonza CC-4147). In the device preparation, the substrate was coated with Collagen (BD 354236) overnight before the cell loading to enhance the cell adhesion. To identify the cell types, the EC was

labelled with orange fluorescent dye (Invitrogen, C2927), while the UM-SCC-1 was labelled by green fluorescent dye (Invitrogen, C2925). Before cell loading, trypsin/EDTA (Gibco 25200) was used to detach cells from their polystyrene culture dishes, and the detached cells were re-suspended at a cell density of 10^5 cells/mL in culture media. The density was chosen for high capture rate and avoiding cell clogging. 100 μL of cell solution was pipetted into the inlet of the microfluidic platform to initiate loading. We mixed two cell types by a ratio of 1:1. This gave a high probability of the pairing of each cell when loaded into the chambers. The culture media was pipetted into the inlet, and the loaded cells were cultured in an incubator. After cell adhesion (one day), the media was replaced with serum free EBM, and the oleic acid (immiscible oil phase) was filled from the left to right by applying a negative pressure (1 psi) to the oil outlet. We changed the media in the media exchange layer every day to supply nutrition to the cells through the semi-permeable membrane under each chamber. At the end of the experiment, the number of living cells was counted by LIVE/DEAD staining (Life Technologies) to acquire quantitative assessment of cell viability and proliferation rates.

Results and discussion:

Cell Capture Mechanism

In order to capture specific number of cells in each culture chamber, a cellular valving mechanism is used.[23-25] In this hydrodynamic capture scheme, two types of flow paths are created in the design: one is a central path and the other is a serpentine path, as shown in Fig. S3 (A). The hydraulic resistance of each path is inversely proportional to its flow rate. The long winding structure of the serpentine path is designed to increase the hydrodynamic resistance, so that the flow rate in this path is lower than that of the central path. Thus, the cells are likely to be guided to the central path and captured. Since the opening of the central path is slightly smaller (Height: 10 μm, Width: 10 μm) than the size of typical mammalian cells, the cells are sterically captured and plug the gap. Once the cell is captured, it blocks the flow in the central path and the remaining cells will flow through the serpentine path and be captured in the next chamber. With proper geometric design, a capture rate of ~90% can be achieved.[25]

To pair cells for the interaction, we designed two capture sites in each chamber. As 90% of individual capture sites capture exactly one cell, the number of captured cells in each chamber is determined by the number of capture sites in the design. As demonstrated by Fig. S3 (B), as the flow resistance of the central path is smaller, the first coming cell is likely to be captured by either capture site. The second coming cell will be captured by the other empty capture site (Fig. S3 (C)). Once both capture sites capture cells, the flow resistance through the central path becomes higher than that of serpentine paths, so the next coming cells will flow through the serpentine paths to the downstream (Fig. S3 (D)). Using this mechanism, we can achieve a high cell-pairing rate in each chamber, and the same mechanism can work for higher number of cells per chamber. As the size of most mammalian cells is similar, there is no selectivity for cell type. Thus, the ratio of captured cells will be similar to the composition of cells in cell solution. For co-culture of two cell types, we loaded a 1:1 ratio of the mixed cells to maximize the probability of 1:1 cell-pairing in the chamber. Fig. 2 (A) shows ten chambers capturing various combinations of cells after cell loading, and four chambers captured a pair of one UM-SCC-1 cell and one endothelial cell. Using two capture sites in each chamber, 25% of chambers capture exact a pair of two cell types, and other combinations can be generated simultaneously (Fig. 2 (B)). The cell behavior of different combinations can be compared side by side in the same device, so the device-to-device variation can be obviated.

Two-phase oil isolation

The immiscibility between oil and water can be an ideal way to isolated microchambers (oil-water two-phase isolation). Previous works demonstrated isolation of water droplets in oil by optimizing channel geometry and hydrophobicity. Pico-liter water droplets can be generated in oil,[26-28] and each single droplet can be used as a nano-lab for cell analysis.[29] Mammalian cells were cultured in droplets, but cell anoikis and media depletion in the droplet limit these technologies only to short term culture (less than one day).[17-19] On the contrary, the conventional media perfusion platforms can allow cell culture longer than two weeks without affecting cell viability.[25] These isolating microenvironments, however, need bulky external components such as pneumatic pumps or function generators for control. In this work, we combine the advantages of these two approaches by integrating immiscible isolation for adherent cell culture and incorporating a semi-permeable membrane under each chamber to allow for continuous media perfusion.[24, 26]

In order to provide high cell viability for the long-term culture in our application, we optimized channel geometry to control the oil flow as shown in the Fig. S4. We designed a higher and wider channel (100 μm by 100 μm) for oil isolation paths and a narrower design (30 μm by 40 μm) for cell loading channels. In this channel configuration, the oil flow, driven by the negative pressure applied, can easily fill the wider channel and thus completely isolate the cell culture chambers, though oil has poorer affinity to the protein-coated hydrophilic channels. It is difficult for oil to invade the cell culture chamber because the collagen coated PDMS is hydrophilic. As a result, the channel geometry can guarantee good oil isolation while protecting cells inside the culture chamber. Fig. 3 shows the immiscible oil isolation process in the channel. A pair of cells were loaded in the chamber as shown in the Fig. 3 (A). When negative pressure was applied from the left, the oil filled the horizontal channels to isolate all the culture chambers. As we balanced the pressure difference between all horizontal channels, isolation process did not affect the cells captured in the chamber (Fig. 3 (B)).

Fabrication of vertical connections by DRIE process

The presented platform has three critical functions: cell capture, oil isolation, and media exchange. To provide the same condition for all chambers on a chip, the symmetry of the channel routing is critical to maintain the pressure balance. However, symmetrical routing for both cell channels, oil channels, and media exchange channels on the same layer is unfeasible. To resolve this problem, we routed the media exchange channels in another layer, and then connect both layers by vertical connections. As the substrate thickness is 100 μm, it is impossible to make small vias (< 200 μm) by isotrpoic hydrogen fluoride (HF) wet etching. To make compact 3D integrated device, deep reactive-ion etching (DRIE) technology (Pagsus Glass etcher) was used instead. We used a fused silica wafer, which is pure silicon dioxide for two reasons: 1) The impurities in glass may interfere with the DRIE process, so it is difficult to achieve a high aspect-ratio deep etching on a glass wafer, and 2) as the fused silica is pure silicon dioxide, it has the same ideal optical and biocompatibility characteristics as glass.[30]

We fabricated different opening sizes, ranging from 25 μm to 300 μm, and all sizes could be etched through by the DRIE process as shown in Fig. 4. The measured etch rate was shown in Fig. 4 (C). The smaller the opening is, the slower the etch rate becomes. However, even for the vias of 25 μm in square, the etch rate was still comparable (~87%) to the larger vias. The process is quite reliable within the range between 25 μm to 300 μm. The size of via connection (25μm x 25μm) that we formed by using a silica wafer is by an order of magnitude smaller than the connections formed through a PDMS membrane (typically ~100 μm), allowing for more compact design.[31,32] The fused silica substrate gives better

mechanical robustness than PDMS thin membrane because it has a higher Young's modulus. Utilizing the presented 3D vertical integration technique, we can eliminate the design constraints of conventional planar fabrication processes and increase the density of integrated chambers in a given area.

Semi-permeable membrane for continuous media renewal and protein accumulation

The small pore size of a semi-permeable membrane allows retaining signaling proteins which typically have a large molecular-weight for cell-cell interaction, while passing the nutrient in the media which typically have a small molecular weight. The semi-permeable membrane is sandwiched between the media exchange layer and the cell-culture chamber. Molecular weights of secreted proteins are typically larger than 10,000 Daltons; therefore, they will accumulate inside the culture chamber, inducing cell-cell interaction. Only the small molecules (e.g., glucose and amino acids) can pass the membrane, allowing continuous nutrient renewal from the media. Fig. 5 shows selective permeability based on molecular weight. The fluorescent dye in Phosphate-buffered saline (PBS, Gibco 10010) was loaded into the cell chamber, and the chamber was isolated by oil. Then, fresh PBS was supplied to the media exchange layer, so we can characterize the diffusion of fluorescent dyes through the semi-permeable membrane as a function of molecular weight by measuring the fluorescent intensity change. We used two different fluorescent dyes in the experiment: a small molecule dye (Fluorescein 5(6)-isothiocyanate, F3651, Sigma-Aldrich, Molecular weight of 389 Daltons) and a large molecule dye (Fluorescein isothiocyanate dextran, FD40S, Sigma-Aldrich, Molecular weight of 40,000 Daltons). Fig. 5 (A-D) demonstrates that the small molecule dye can diffuse through the semi-permeable membrane to the media exchange layer and then be washed away. The fluorescent intensity reduced to 27% from the initial intensity after 60 minutes. On the contrary, Fig. 5 (E-H) shows that the large molecule dye can be retained inside the chamber. After 60 minutes, the fluorescent intensity only reduced by 8%. Fig. 5(I) plots the change of relative fluorescent intensity for two different dyes, respectively. It clearly shows the selective permeability for different molecule sizes, demonstrating the feasibility to continuous media renewal in the presented co-culture platform.

Proliferation enhancement by cell-cell interaction

As a proof of concept, we demonstrated cell interaction between UM-SCC-1 (head and neck squamous cell carcinoma) cells and endothelial cells (EC). Endothelial cells are known to secrete a number of growth factors that enhance the growth of tumors.[33] We compared co-culture of one UM-SCC-1 and one EC with single cell culture of one UM-SCC-1. After cell loading, the chambers were isolated utilizing the immiscible oil for three days. In the chamber loaded with the EC, the secreted cytokines from the EC were accumulated over time and boosted the growth of the UM-SCC-1. Fig. 6 shows the proliferation results after three days. The isolated single tumor cell barely proliferated (Fig. 6 (A)), while the UM-SCC-1 cell co-cultured with one EC proliferated to three cells (Fig. 6 (B)). The proliferation rate of the co-cultured UM-SCC-1 cells was twice that of the isolated UM-SCC-1 cells (Fig. 6 (C)). Both isolated and co-cultured UM-SCC-1 cells showed good cell viability, implying stable nutrition supply through the semi-permeable membrane (Fig. 6 (D)) during the course of the experiments. By exchanging nutrition through the membrane, the presented platform can maintain the cell viability of 75% up to 7 days for longer experiments. These preliminary results successfully demonstrated the capability of our device retaining the secreted factors for interaction while providing stable media perfusion through semi-permeable membrane to maintain good cell viability.

Conclusions

We have successfully implemented a cell-cell interaction platform that can be used to co-culture a pair of cells in one chamber. The platform attains a high cell pairing rate of 25% and reliable chamber isolation by immiscible two-phase flows using oil. Although chambers are isolated, the nutrition can be supplied through a semi-permeable membrane, while the secreted signaling proteins can be retained inside the chamber for cell-cell interaction. The membrane selectivity based on molecular weights was verified utilizing fluorescent dyes. We achieved a compact integration of co-culture chamber arrays by stacking double layers through vertical via connections in the silica substrate. In the current chip, 56 chambers were implemented for proof of concept and we believe it can be easily extended to 1,000 chambers for high-throughput assays. The preliminary experiments have confirmed the increase in proliferation of cancer cells when co-cultured with endothelial cells, demonstrating the feasibility of the proposed microfluidic platform for studying tumor-stromal interaction by controlling microenvironments in cell niches.

Acknowledgement

This work was supported in part by the Department of Defense (W81XWH-12-1-0325) and in part by the National Institute of Health (1R21CA175857).

Captions:

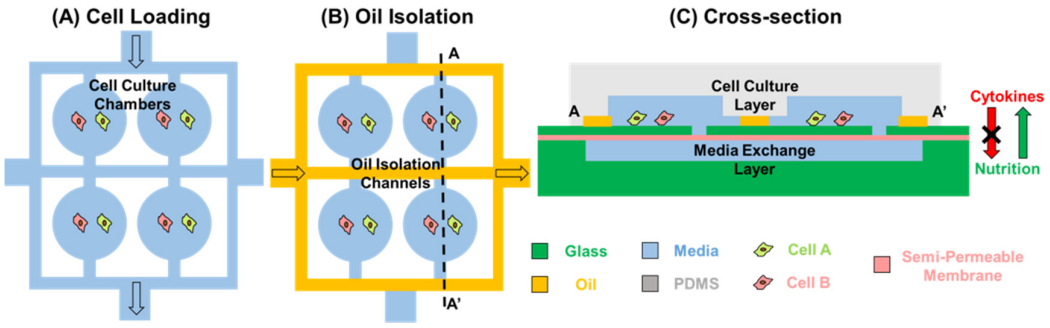

Fig. 1. Schematics of the proposed cell-niche-on-chip. (A) Cells are loaded and captured in each chamber by paring with different types of cell. (B) Oil is introduced from left to right in the upper layer to isolate the culture chambers by immiscible oil. (C) Illustration of cross-sectional view of the device shows that secreted cytokines are accumulated inside the chamber for cell-cell interaction, while the nutrition can be steadily supplied through a semi-permeable membrane.

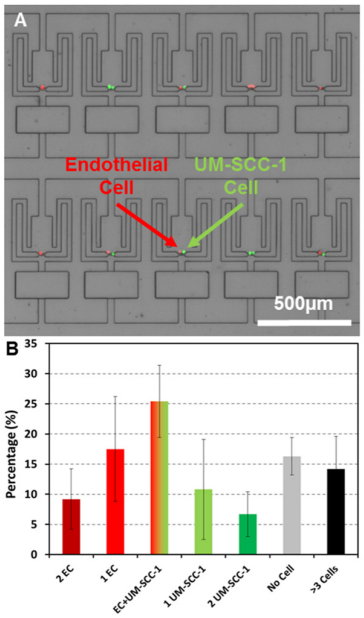

Fig. 2. Multiple cells captured in a chamber: (A) Capturing of different combinations of UM-SCC-1 and endothelial cells (EC), and (B) the capture rate of different cell combinations in an array of chambers with two capture sites when loading the mixed cells of UM-SCC-1 and EC at a 1:1 ratio.

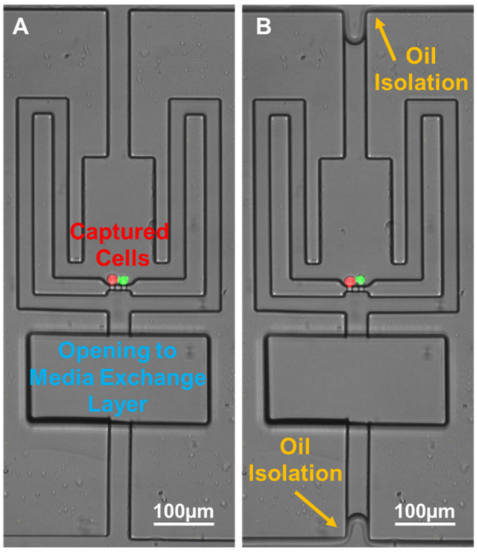

Fig. 3. Oil isolation: (A) before and (B) after oil introduction. The culture chamber forms an isolated microenvironment, and the oil isolation process does not affect the cells cultured in the chamber.

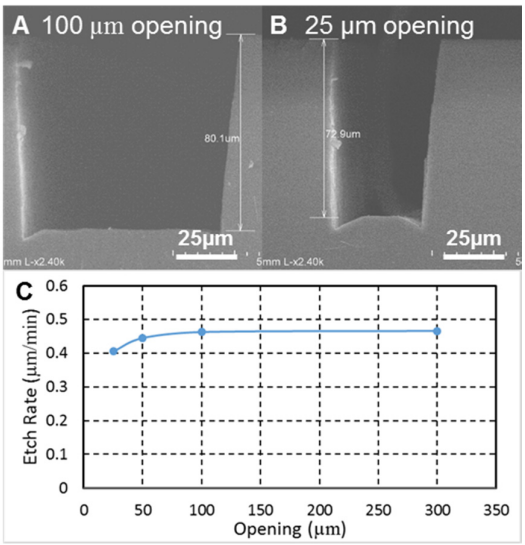

Fig. 4. Fabrication of vertical connections by DRIE: (A) the scanning electron microscope (SEM) of a 100 μm opening connection, (B) the SEM of a 25 μm opening connection, and (C) The etch rate of fused silica with different sizes of opening.

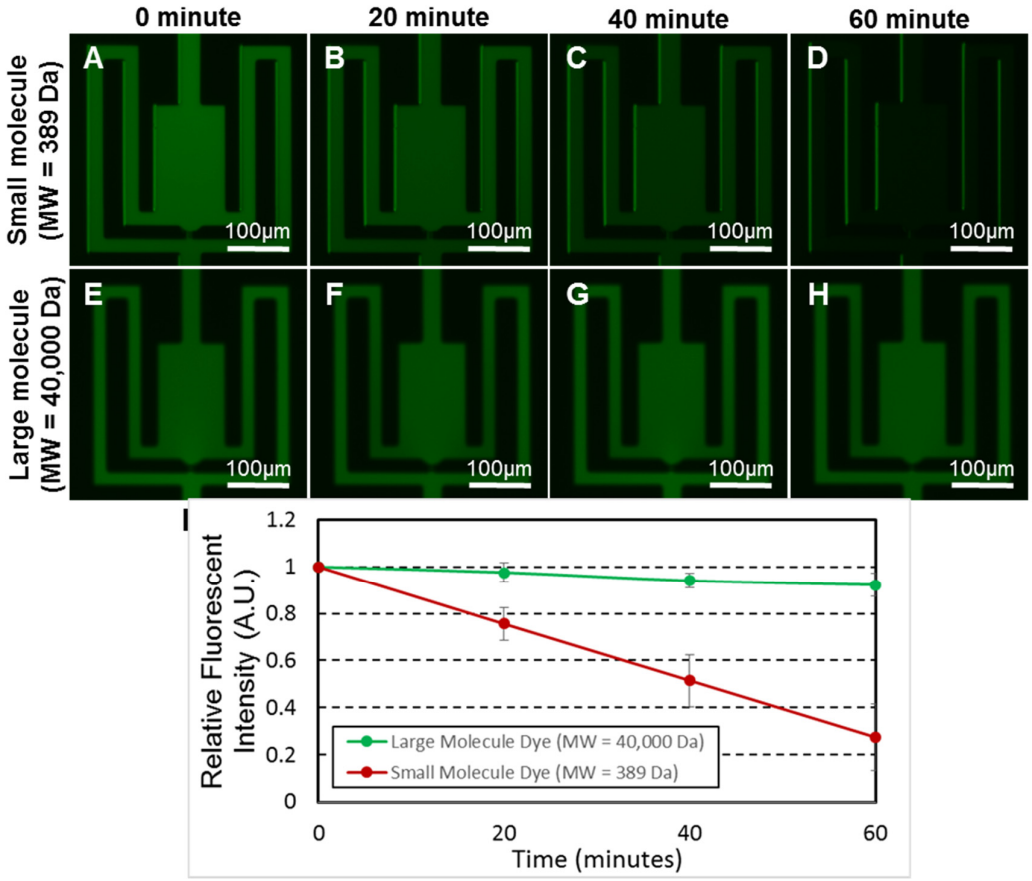

Fig. 5. The selectivity of retaining fluorescent dyes based on molecular weights. (A-D) Small molecule dye (MW = 389 Da) was gradually diffused out through a semi-permeable membrane: (A) initial fluorescent intensity, (B) fluorescent intensity after 20 minutes, (C) after 40 minutes, and (D) after 60 minutes. (E-H) Large molecule dye (MW = 40,000 Da) was retained in the chamber: (E) initial fluorescent intensity, (F) fluorescent intensity after 20 minutes, (G) after 40 minutes, and (H) after 60 minutes. (I) The plot of relative fluorescent intensity of fluorescent dyes in the chamber over time. The results clearly demonstrate that the small molecules (e.g., glucose, amino acids) can be exchanged, while the large molecules (e.g., signaling proteins) can be retained in the chamber for interaction (N = 5 chambers).

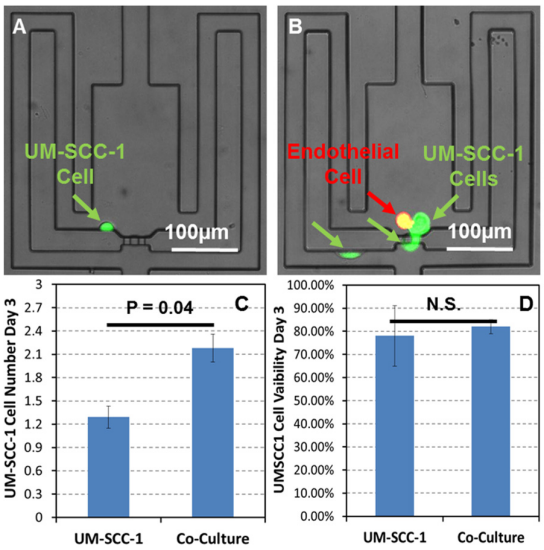

Fig. 6. Cell Interaction between UM-SCC-1 and EC for three days. (A) A single UM-SCC-1 cell after 3-day culture in the chamber. No proliferation was observed. (B) A pair of one UM-SCC-1 and one EC co-cultured for 3 days. After three days, one UM-SCC-1 cell became three cells. (C) The comparison between the proliferation rate of single UM-SCC-1 cell and the co-cultured EC - UM-SCC-1 cells. The result shows that the EC can enhance the proliferation of UM-SCC-1 cell. Data points represent means ± standard deviations (N = 4 devices), P = 0.04. (D) Viability of UM-SCC-1 in the chamber after 3-day culture shows that the cells were healthy in both cases. Data points represent means ± standard deviations (N = 4 devices), and no significant difference was observed.

References:

[1] R. Peerani and Peter W. Zandstra*, J. Clin. Invest*, 2010, **120**, 60–70.

[2] D. Hanahan, R. A. Weinberg. *Cell*, 2011, **144**, 646-74.

[3] M. Cristofanilli, G. T. Budd, M. J. Ellis, A. Stopeck, J. Matera, M. C. Miller, J. M. Reuben, G. V. Doyle, W. J. Allard, L. W.M.M. Terstappen, and D. F. Hayes*, N Engl J Med*, 2004, **351**, 781-91.

[4] M. J. Bissell and W. C Hines, *et al, Nature Medicine*, 2011, **17**, 320-329.

[5] P. Mignatti, T. Morimoto, D.B. Rifkin, *Proc Natl Acad Sci U S A*, 1991, **15**, 11007-11.

[6] A.Y. Hsiao, Y. Torisawaa, Y. Tung, S. Sud, R. S. Taichman, K. J. Pienta, , S. Takayamaa*, Biomaterials*, 2009, **30**, 3020-7.

[7] M. Bauer, G. Su, D. J. Beebe, A. Friedl, *Integr Biol.* , 2010, **2**, 371-8.

[8] Y. Gao, D. Majumdar, B. Jovanovic, C. Shaifer, P. C. Lin. A. Zijlstra, D. J. Webb and D. Li*, Biomed Microdevices*, **13**, 539-48, 2011.

[9] D. Majumdar, Y. Gao, D. Li, and D. J. Webb*, J Neurosci Methods*, **196**, 38-44, 2011.

[10] M. Heneweer, M. Muusse, M. Dingemans, P. C. de Jong, M. van den Berg, J. T. Sanderson, *Toxicol Sci*., 2005, **83**, 257-63.

[11] J. Park, H. Koito, J. Li, A. Han, Biomed *Microdevices*, 2009, **11**, 1145-53.

[12] H. Ma, T. Liu, J. Qin, B. Lin, *Electrophoresis*, 2010, **31**, 1599-605.

[13] 13 Elliot E. Hui, Proc. Natl. Acad. Sci. U. S. A, 2007, 104, 5722–5726.

[14] I. K. Zervantonakis, S. K. Hughes-Alford, J. L. Charest, J. S. Condeelis, F. B. Gertler and R. D. Kamm, roc. Natl. Acad. Sci. U. S. A., 2012, 109, 13515–20.

[15] E. Tumarkin, L. Tzadu, E. Csaszar, M. Seo, H. Zhang, A. Lee, R. Peerani, K. Purpura, P. W. Zandstra and E. Kumacheva*, Integr. Biol, 2011,* **3**, 653-662.

[16] S. Hong, Q. Pan and L. P. Lee, *Integr. Biol.,* 2012, **4**, 374–80.

[17] J. Pan, A. L. Stephenson, E. Kazamia, W. T. S. Huck, J. S. Dennis, A. G. Smith and C. Abell*, Integr. Biol.*, 2011*,* **3**, 1043–1051.

[18] T. P. Lagus and J. F. Edd, RSC Adv, 2013, **3**, 20512.

[19] A. Huebner, D. Bratton, G. Whyte, M. Yang, A. J. deMello, C. Abell and F. Hollfelder, Lab Chip, 2009, **9**, 692–698.

[20] S.M. Frisch, R.A. Screaton,Curr Opin Cell Biol, 2001 **13**, 555-562.

[21] P. Ingram, Y. J. Kim, T. Bersano-Begey, X. Lou, A. Asakura, and E. Yoon, *Proceeding of MicroTAS*, 2010, 277-279.

[22] Y.-C. Chen, X. Lou, P. Ingram, and E. Yoon, *Proceeding of MEMS*, 2012, 792-795.

[23] W.-H. Tan and S. Takeuchi *Proc Natl Acad Sci U S A*, 2007, 104(4), 1146–1151.

[24] J. Chung, Y. J. Kim and E. Yoon, *Appl. Phys. Lett,* 2011, **12**, 3701-3703.

[25] Y.-C. Chen, P. Ingram, X. Lou, and E. Yoon, *Proceeding of MicroTAS*, 2012, 1241-1244.

[26] S.-Y. The, R. Lin, L.H. Hung and A.P. Lee. *, Lab Chip*, 2008, **8**, 198–220.

[27] W.-A. C. Bauer, M. Fischlechner, C. Abell and W. T. S. Huck, *Lab Chip*, 2010, **10**, 1814–1819.

[28] W.-H. Tan and S. Takeuchi*, Lab Chip*, 2006, **6**, 757–763.

[29] M.T. Guo, A. Rotem, J. A. Heyman, D. A Weitz*, Lab Chip*, 2012, **12**, 2146–2155.

[30] Z. Cao, B. VanDerElzen, K. J. Owen, J. Yan, G. He, R. L. Peterson, D. Grimard, and K. Najafi, *Proceeding of MEMS*, 2013, 361-364

[31] M. Zhang, J. Wu, L. Wang, K. Xiao and W. Wen, *Lab Chip*, 2010, **10**, 1199-1203

[32] J M. Karlsson1, T. Haraldsson, C. F. Carlborg, J. Hansson, A. Russom and W. VanDerWijngaart, *J. Micromech. Microeng*. 2012, 22, 085009.

[33] K. G. Neiva, K. A. Warner, M. S. Campos, Z. Zhang, J. Moren, T. E. Danciu and J. E. Nör BMC Cancer 2014, **14**, 99